PCCP

PAPER

View Article Online
View Journal | View Issue

Cite this: *Phys. Chem. Chem. Phys.*, 2019, **21**, 21104

Synthesis of nanosized vanadium(v) oxide clusters below 10 nm†

Maximilian Lasserus, [a] Daniel Knez, [b] Florian Lackner, [a] Martin Schnedlitz, [a] Roman Messner, [a] Daniel Schennach, [a] Gerald Kothleitner, [b] Ferdinand Hofer, [b] Andreas W. Hauser *[a] and Wolfgang E. Ernst *[a]

Received 6th August 2019,
Accepted 9th September 2019

DOI: 10.1039/c9cp04357h

rsc.li/pccp

Vanadium oxide clusters with a mean diameter below 10 nm are investigated by high resolution Scanning Transmission Electron Microscopy (STEM), Electron Energy Loss Spectroscopy (EELS) and UV-vis absorption spectroscopy. The clusters are synthesised by sublimation from bulk vanadium(v) oxide, in combination with a pick-up by superfluid helium droplets. The latter act as reaction chambers which enable cluster growth under fully inert and solvent-free conditions. High-resolution STEM images of deposited vanadium oxide particles allowing for the determination of lattice constants, clearly indicate a dominating presence of V_2O_5. This finding is further supported by UV-vis absorption spectra of nanoparticles after deposition on fused silica substrates, which indicates that the oxidation state of the material is preserved over the entire process. From the results of the UV-vis measurement, the band gap of the nanosized V_2O_5 could be determined to be 3.3 eV. The synthesis approach provides a route to clean V_2O_5 clusters as it does not involve any surfactant or solvents, which is crucial for an unbiased measurement of intrinsic catalyst properties.

1 Introduction

Interest in nanometer-sized metal oxide particles has been increasing in the last decades due to their numerous applications in catalysis, medicine, energy storage, electronics and optics.[1,2] When the diameters of such particles approach the sub 10 nm regime, the surface-to-volume ratio increases dramatically. The higher fraction of atoms at edges and corners reduces the mean coordination number, which enhances their chemical reactivity.[3] Transition metal oxides have unique properties originating from the characteristics of the outer d-band electrons. Vanadium oxide is a prominent representative of this group of materials, and clusters consisting of it have been object of active research due to their numerous oxidation states and the relatively high abundance of the material. Theoretical and experimental studies of the structure and stability of small clusters of V_2O_5 have been performed by Sauer *et al.*[4–7] Regarding strategies for a controlled synthesis of nanostructures, Limberg *et al.* showed that thin films of V_2O_5 can be obtained by vapour deposition of heated V_2O_5 powder.[8] However, to the knowledge of the authors, none of the current techniques allows for a controlled coating with V_2O_5 nanoparticles. Among the possible applications, heterogeneous catalysis is probably the most important field,[9–13] but recent research efforts have also been dedicated to energy storage.[14]

For the synthesis of small ($\leq$10 nm) transition metal oxide clusters, solution based methods are often used, such as sol–gel techniques, microemulsions, micelle/reverse micelle methods or precipitation.[15–23] A disadvantage of all these techniques is the inevitable impact onto the product shape, structure and purity. An alternative approach is based on the evaporation of vanadium oxide with lasers, but has undesired side effects such as the production of highly reactive fragments, charged complexes and other unwanted by-products.[24,25]

In this paper we employ a different strategy to synthesise nanoparticles which is based on the accumulation of V_2O_5 oligomers in helium nanodroplets. The present work expands our previous experiments from the *in situ* characterisation of V_2O_5 oligomers in a helium droplet beam,[26] towards the formation of nanoparticle films comprising of individually deposited particles with diameters below 10 nm. After deposition, several *ex situ* measurement techniques can be applied to the particles in order to reveal their characteristics on different supports.

The synthesis method has its origin in spectroscopy,[27] where helium droplets have been used to assemble and investigate elusive molecules,[28] and has evolved into a versatile method for the production and subsequent deposition of metal clusters.[29,30] Using the helium droplet method for the synthesis of transition

[a] *Institute of Experimental Physics, Graz University of Technology, Petersgasse 16, A-8010 Graz, Austria. E-mail: andreas.w.hauser@gmail.com, wolfgang.ernst@tugraz.at; Fax: +43 (316) 873-108140; Tel: +43 (316) 873-8157, +43 (316) 873-8140*

[b] *Institute for Electron Microscopy and Nanoanalysis & Graz Centre for Electron Microscopy, Graz University of Technology, Steyrergasse 17, A-8010 Graz, Austria*

† Electronic supplementary information (ESI) available. See DOI: 10.1039/c9cp04357h

metal oxide clusters is a novel exertion of this well known synthesis technique and is a new step towards understanding of these highly interesting materials.

2 Experimental section

The experimental setup used for the synthesis of V_2O_5 clusters is described in detail in ref. 30. A short overview is given in the following. High purity helium gas (99.9999%) is expanded through a cooled 5 μm nozzle under a constant pressure of 20 bar into high vacuum ($\approx 5 \times 10^{-5}$ mbar), whereby helium droplets are formed. Depending on the nozzle temperature, different size distributions of droplets are accessible. In our experiment the nozzle temperature has been set to 5.4, 6.7 and 8 K, which corresponds to average sizes of 1.68×10^{10}, 1 to 6×10^7 and 5.31×10^6 helium atoms per droplet, respectively.[32] For each temperature, a deposition time of ≈20 minutes was chosen. After the expansion the helium beam is cropped by a 400 μm skimmer before entering the next vacuum chamber with a pressure of $\approx 5 \times 10^{-6}$ mbar during deposition. Here, vanadium(v) oxide (V_2O_5, Matek Prod. No. 008133) with a purity of 99.9% is placed in a quartz crucible (Kurt Lesker EVC2Q), surrounded by a tungsten heating basket (Kurt Lesker EVB8B3030W), and is resistively heated to temperatures between 1100 K and 1200 K. When heated, the vapour pressure of the desired material rises, creating a pick-up zone above the basket. As documented in ref. 26, small oligomers of vanadium pentoxide, preferably units of V_4O_{10}, tend to evaporate from the V_2O_5 powder upon heating. After collision with a helium droplet, these units of sublimated V_2O_5 remain attached and agglomerate to V_2O_5 clusters inside the droplet. The energy released in the process of bond formation during cluster aggregation is dissipated by the evaporation of helium atoms (approximately 5 cm^{-1} per He atom).[33] This evaporation is monitored by a residual gas analyser (Balzer QMA 200/QME 200) by comparing the He signal before and during evaporation, providing a convenient way to monitor the doping level. After the pick-up chamber the helium droplet beam is again cropped by a 2 mm skimmer before it enters the measurement chamber, with a pressure of $\approx 1 \times 10^{-8}$ mbar, during deposition. In this last chamber the clusters are deposited onto TEM grids. Additional diagnostic tools are installed to characterise the doped droplet beam.[30]

2.1 Scanning transmission electron microscopy

After deposition on amorphous carbon grids under soft landing conditions,[34] the sample is exposed to ambient air during transport (≈10 min) and insertion into a Scanning Transmission Electron Microscope (STEM), where the V_2O_5 particles are studied *via* a high-angular annular dark-field (HAADF) imaging detector at atomic resolution using a probe-corrected FEI Titan^3 G2 60-300 TEM. The microscope was operated at 300 keV achieving a resolution of ≈70 pm. A Gatan quantum energy filter, attached to the microscope, is employed for electron energy loss spectroscopy (EELS).

Vanadium has several stable oxides and a transition between them can be easily induced *e.g.* by temperature increase or by electron irridation. The reducing effect of the electron beam during STEM measurements, in particular for nanostructured objects, is well known and also documented for the case of vanadium oxides.[35] In order to avoid any undesired reduction under the electron beam, the dose is kept as low as possible by using an electron current of 100 pA and short exposure times for each particle.[36]

2.2 UV-vis absorption spectroscopy

UV-vis absorption spectra were measured using a Shimadzu UV-1800 spectrophotometer. The V_2O_5 nanoparticles were deposited on a fused silica microscope slide (Corning 7980, fused silica, 1 mm thickness). After deposition the slide was taken out of vacuum and placed into the spectrometer to acquire the shown spectra. A second fused silica slide from the same patch was used as reference.

3 Results

3.1 STEM

A High Angle Annular Dark Field (HAADF) overview image of clusters is shown in Fig. 1. Several bright nanostructures are

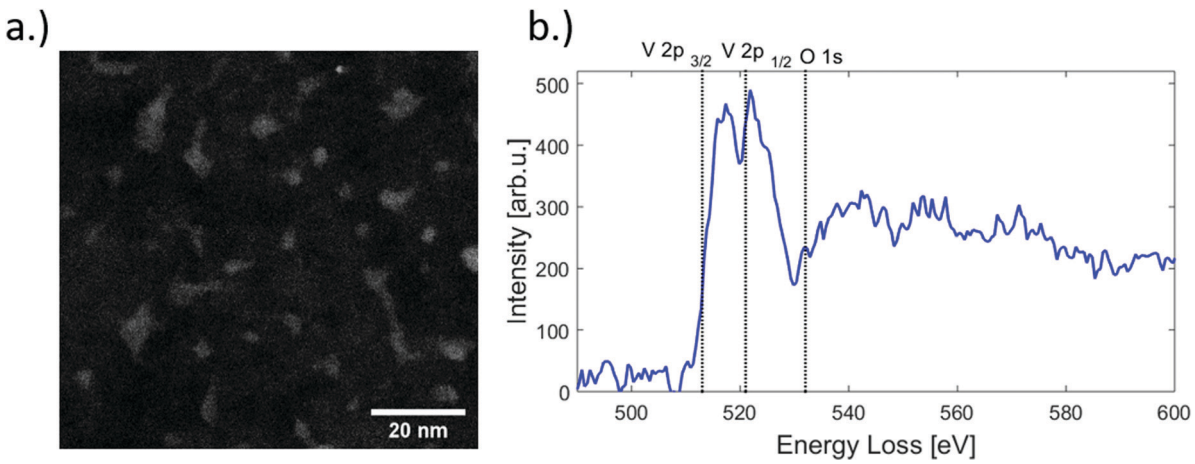

Fig. 1 (a) HAADF image of V_2O_5 structures as seen in STEM, for cold head temperatures of 8, 6.7 and 5.4 K and deposited on one substrate. (b) EELS spectrum of a selected nanoparticle. The characteristic V-L_2, V-L_3 and the O-K edges are indicated by vertical dashed lines.[31]

distinguishable. Note that some elongated shapes are also visible (see in Fig. 1 in the right lower corner), which is a typical side effect of our synthesis method. In larger helium droplets, created at nozzle temperatures below 8 K, metal clusters become elongated due to the presence of one-dimensional vortices inside the superfluid helium droplets along which the dopants preferentially agglomerate.[37–39]

The shape and size of the deposited nanostructures is revealed directly by the STEM images and can be explained by the He synthesis given certain helium droplet source conditions. However, a more challenging task is the determination of the oxidation state, *i.e.* the actual structural composition of the vanadium oxide after deposition. Electron energy loss spectroscopy (EELS) is an element-sensitive technique that can provide insights into the oxidation states of a material and is routinely employed for this purpose in transmission electron microscopy. The approach relies on the fact that near edge features as observed in EELS spectra are highly sensitive to the local valence electronic structure, which depends on the nature of chemical bonds in the material, in our case, the various types of V–O bonds in the nanoparticles. However, although EELS has been successfully employed in previous experiments on bulk vanadium oxide as well as thin films,[40–42] in this particular case the approach turned out to be futile due to the close proximity of the V L- and O K-edges. The low electron beam dosage mentioned above, a necessity to avoid particle damage and to prevent electron-beam induced reduction,[43] provides a rather weak EELS signal and a relatively low resolution compared to other published spectra. An EELS spectrum obtained from a nanoparticle is presented in Fig. 1, showing the L2 (V $2p_{1/2}$) and L3 (V $2p_{3/2}$) main features peaking at 517.1 and 522.7 eV, respectively. The V 2p L-edges as well as the O 1s K-edge are indicated by a vertical dashed line. However, due to the large number of possible oxidation states and the similarity in the EELS signal a distinct characterisation is not possible. A more detailed discussion of the EELS signal is provided in the ESI.†

As an alternative method to reveal the oxidation state, the lattice constants of the clusters were measured directly from HAADF images and compared to bulk values. In order to do that, TEM images have been selected where suitable vanadium oxide particles with multiple grains were visually accessible at the same time.

In these cases, different lattice reflexes could be determined within the same particle, and the lattice constants could be derived as indicated in Fig. 2, where regions of sufficient lattice contrast are highlighted. The red lines mark a group of lattice planes with a distance of 2.7 Å which can be assigned to the (011) plane of V_2O_5, while the blue lines mark a region in which the lattice reflexes have a spacing of 2.2 Å, which can be assigned to the (020) plane of V_2O_5. Another structure is presented in Fig. 3, where a lattice spacing of 5.7 Å could be measured, which we assign to the (200) plane of V_2O_5.[44] For the sake of a direct comparison we plotted the known lattice constants of the vanadium oxides in Fig. 4 together with the measured distances from Fig. 3 and Fig. 2.[45–49] The displayed reflexes are derived from the published lattice parameters using

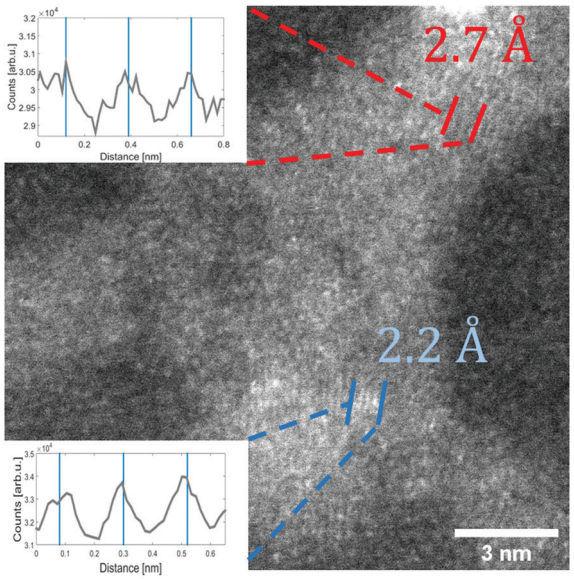

Fig. 2 STEM HAADF image of a V_2O_5 particle (synthesised at 5.4 K cold head temperature). Two regions are marked where lattice constants could be extracted from the image. The respective intensity profile between the lines is shown in the inset. The black lines indicate a group of planes with a spacing of 2.7 Å the blue lines mark a group of planes with a spacing of 2.2 Å.

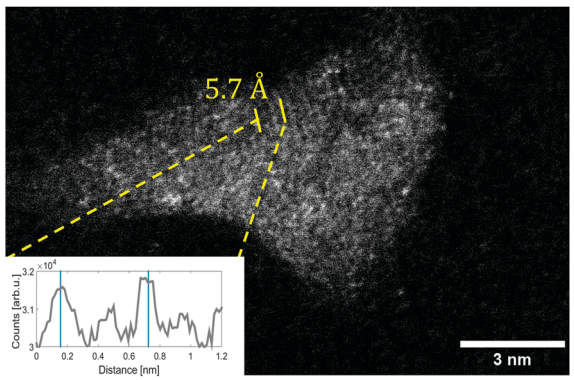

Fig. 3 STEM HAADF image of a V_2O_5 structure (synthesised at 5.4 K cold head temperature). The intensity profile of the local structure between the yellow lines is shown in the left corner. The distance of the peaks is marked by blue lines indicating the lattice distance of 5.7 Å.

the software Vesta.[50] The coloured area mimics the uncertainty of the microscope and therefore indicates the possible reflexes of each oxide. Hereby, the only oxide offering significant lattice reflexes in all marked regions is V_2O_5. Within the recorded images, we did not find a lattice distance between 4 and 4.5 Å. The lack of these reflexes may be due to the limited number of clusters with respective lattice orientations observable during the experiment. However, together with our spectral observation (see below) we consider the result as strong evidence for that the oxidation state of the nanoparticles is preserved, starting from their growth in the He droplets from sublimated V_2O_5 fragments, up to their final deposition on the support.

The size distribution of the V_2O_5 clusters was determined by analysing the HAADF images. A total of 523 clusters has been

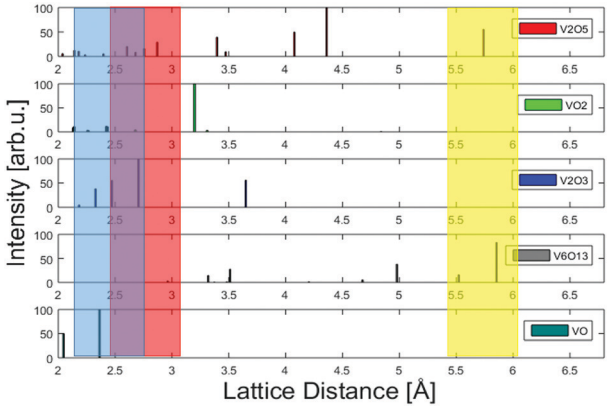

Fig. 4 A comparison of lattice constants for various vanadium oxides. The measured lattice constants derived from Fig. 2 and 3 and their uncertainty due to the limited resolution are represented by the coloured areas. The colours represent the respective marking in each figure. By comparison to known, much better resolved peak positions taken from powder diffraction measurements, V_2O_5 is identified as the most likely oxide.[45–49]

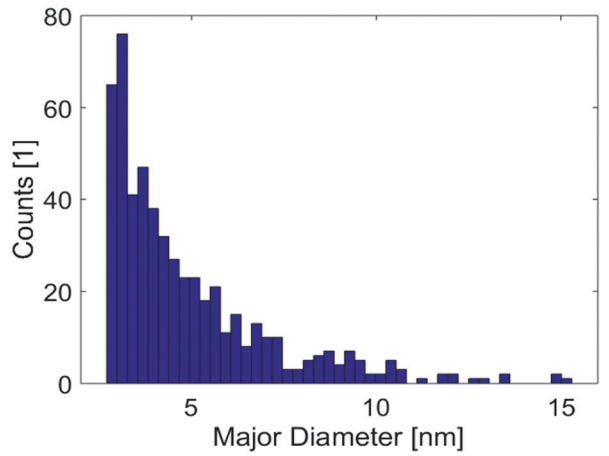

Fig. 5 Size distribution of V_2O_5 clusters derived from HAADF images providing a total cluster count of 523. 'Major diameter' refers to the longest distance within a cluster. A cutoff below 2 nm was used to exclude noise. This is the total size distribution from the deposition at nozzle temperatures of 8, 6.7 and 5.4 K on one substrate.

investigated to produce a typical log-norm distribution as shown in Fig. 5. The larger part of the synthesised clusters has a size below 10 nm.

3.2 UV-vis absorption spectroscopy

To determine the dominant oxidation state of the deposited clusters, UV-vis absorption spectroscopy serves as an additional method for the investigation of the chemical composition of the V_2O_5 particles. In Fig. 6(a) the clusters show a strong absorption in the UV region, but are transparent in the visible and IR regime. The recorded spectrum agrees well with the absorption spectrum of V_2O_5, which, among all the previously studied vanadium oxides, is the only species that exhibits no absorption in the visible.[2] This can be seen clearly from Fig. 6(b) which contains a direct comparison to spectra taken

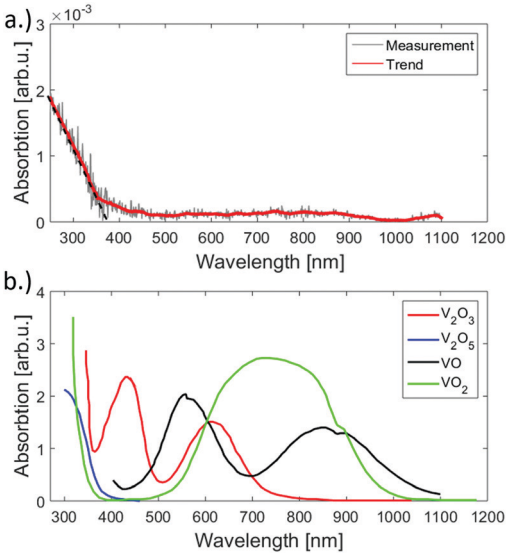

Fig. 6 UV-vis absorption spectra of the synthesised V_2O_5 clusters on fused silica (a) and reference spectra taken from ref. 2 (b). An absorption near the ultraviolet region is evident for the measured signal. The spectrum was acquired by subtracting the signal of a plane spot at the support and the spot of cluster deposition. When comparing the reference spectra to the measurement, the similarity to the V_2O_5 is visible.

from ref. 2. The band gap of the prepared samples has been determined as 375 nm (3.3 eV) from a line-fit to the decreasing absorption in the UV, indicated in Fig. 6 (dashed line). The value is higher than the reported value of bulk (2.3 eV, see ref. 51) but smaller than the HOMO–LUMO gap known for the molecular $(V_2O_5)_2$ dimer (4.4 eV, see ref. 52). As clusters in the sub 10 nm regime are bridging the gap between bulk and molecules, it appears reasonable that the obtained value resides between these two cases.

4 Conclusion

V_2O_5 clusters with a size distribution $\leq$10 nm have been synthesised through sublimation from bulk, helium-assisted growth and follow-up deposition. EELS measurements confirm the presence of vanadium, but did not provide further information on oxidation states. Therefore, the chemical stoichiometry of the synthesised clusters was determined based on lattice distances as measured from HAADF images. We find best agreement with reflexes of vanadium(v) oxide, a suggestion which is further confirmed by UV-vis absorption measurements. In the course of the latter also a band gap of 3.3 eV could be determined for nanostructured V_2O_5 clusters with average sizes below 10 nm. This confirms that the chosen way of particle synthesis through helium droplets does not affect the chemical composition of V_2O_5, which suggests future combinations with other metal impurities during synthesis in order to produce application-tuned nanostructured catalyst materials.

Conflicts of interest

There are no conflicts to declare.

Acknowledgements

This research has been supported by the Austrian Science Fund (FWF) under Grant FWF PIR8-N34. Further support by NAWI Graz is gratefully acknowledged. F. L. and R. M. acknowledge support by the Austrian Science Fund (FWF) under Grant FWF P30940-N36. We thank the Institute of Solid State Physics at Graz University of Technology for providing helpful discussion and access to the UV-vis spectrophotometer.

References

1 J. L. G. Fierro, *Metal oxides: chemistry and applications*, CRC Press, 2005.
2 N. H. Choi, S.-k. Kwon and H. Kim, *J. Electrochem. Soc.*, 2013, **160**, A973–A979.
3 E. Roduner, *Chem. Soc. Rev.*, 2006, **35**, 583–592.
4 K. R. Asmis and J. Sauer, *Mass Spectrom. Rev.*, 2007, **26**, 542–562.
5 K. R. Asmis, G. Meijer, M. Brümmer, C. Kaposta, G. Santambrogio, L. Wöste and J. Sauer, *J. Chem. Phys.*, 2004, **120**, 6461–6470.
6 K. R. Asmis, G. Santambrogio, M. Brümmer and J. Sauer, *Angew. Chem., Int. Ed.*, 2005, **44**, 3122–3125.
7 S. Guimond, M. A. Haija, S. Kaya, J. Lu, J. Weissenrieder, S. Shaikhutdinov, H. Kuhlenbeck, H.-J. Freund, J. Döbler and J. Sauer, *Top. Catal.*, 2006, **38**, 117–125.
8 C. Herwig and C. Limberg, *Inorg. Chem.*, 2008, **47**, 2937–2939.
9 G. Busca, L. Lietti, G. Ramis and F. Berti, *Appl. Catal., B*, 1998, **18**, 1–36.
10 G. Centi, *Appl. Catal., A*, 1996, **147**, 267–298.
11 G. Deo and I. E. Wachs, *J. Catal.*, 1994, **146**, 323–334.
12 Q. Sun, J.-M. Jehng, H. Hu, R. G. Herman, I. E. Wachs and K. Klier, *J. Catal.*, 1997, **165**, 91–101.
13 C. Resini, T. Montanari, G. Busca, J.-M. Jehng and I. E. Wachs, *Catal. Today*, 2005, **99**, 105–114.
14 J. Barker, M. Saidi and J. Swoyer, *J. Electrochem. Soc.*, 2003, **150**, A1267–A1272.
15 D. Wang, T. Xie and Y. Li, *Nano Res.*, 2009, **2**, 30–46.
16 R. Gvishi, *J. Sol-Gel Sci. Technol.*, 2009, **50**, 241.
17 S. G. Kwon and T. Hyeon, *Acc. Chem. Res.*, 2008, **41**, 1696–1709.
18 C. Rao, S. Vivekchand, K. Biswas and A. Govindaraj, *Dalton Trans.*, 2007, 3728–3749.
19 B. Chaudret and K. Philippot, *Oil Gas Sci. Technol.*, 2007, **62**, 799–817.
20 J. K. Lim, S. A. Majetich and R. D. Tilton, *Langmuir*, 2009, **25**, 13384–13393.
21 J. Tang, F. Redl, Y. Zhu, T. Siegrist, L. E. Brus and M. L. Steigerwald, *Nano Lett.*, 2005, **5**, 543–548.
22 B. L. Cushing, V. L. Kolesnichenko and C. J. O'Connor, *Chem. Rev.*, 2004, **104**, 3893–3946.
23 J. Rockenberger, E. C. Scher and A. P. Alivisatos, *J. Am. Chem. Soc.*, 1999, **121**, 11595–11596.
24 D. E. Bergeron, A. W. Castleman, N. O. Jones and S. N. Khanna, *Nano Lett.*, 2004, **4**, 261–265.
25 K. Molek, Z. Reed, A. Ricks and M. Duncan, *J. Phys. Chem. A*, 2007, **111**, 8080–8089.
26 M. Lasserus, M. Schnedlitz, R. Messner, F. Lackner, W. E. Ernst and A. W. Hauser, *Chem. Sci.*, 2019, **10**(12), 3473–3480.
27 J. P. Toennies and A. F. Vilesov, *Angew. Chem., Int. Ed.*, 2004, **43**, 2622–2648.
28 C. Callegari and W. E. Ernst, in *Handbook of High Resolution Spectroscopy*, ed. F. Merkt and M. Quack, John Wiley & Sons, Chichester, 2011.
29 A. Boatwright, C. Feng, D. Spence, E. Latimer, C. Binns, A. M. Ellis and S. Yang, *Faraday Discuss.*, 2013, **162**, 113–124.
30 P. Thaler, A. Volk, D. Knez, F. Lackner, G. Haberfehlner, J. Steurer, M. Schnedlitz and W. E. Ernst, *J. Chem. Phys.*, 2015, **143**, 134201.
31 N. Pinna, M. Willinger, K. Weiss, J. Urban and R. Schlögl, *Nano Lett.*, 2003, **3**, 1131–1134.
32 L. F. Gomez, E. Loginov, R. Sliter and A. F. Vilesov, *J. Chem. Phys.*, 2011, **135**, 154201.
33 A. Bartelt, J. Close, F. Federmann, N. Quaas and J. Toennies, *Phys. Rev. Lett.*, 1996, **77**, 3525.
34 M. P. de Lara-Castells, N. F. Aguirre, H. Stoll, A. O. Mitrushchenkov, D. Mateo and M. Pi, *Communication: Unraveling the 4He droplet-mediated soft-landing from ab initio-assisted and time-resolved density functional simulations: Au@4He300/TiO2(110), 2015.*
35 D. S. Su, M. Wieske, E. Beckmann, A. Blume, G. Mestl and R. Schlögl, *Catal. Lett.*, 2001, **75**(1–2), 81–86.
36 D. Knez, M. Schnedlitz, M. Lasserus, A. Schiffmann, W. E. Ernst and F. Hofer, *Ultramicroscopy*, 2018, **192**, 69–79.
37 E. Latimer, D. Spence, C. Feng, A. Boatwright, A. M. Ellis and S. Yang, *Nano Lett.*, 2014, **14**, 2902–2906.
38 M. Schnedlitz, M. Lasserus, D. Knez, A. W. Hauser, F. Hofer and W. E. Ernst, *Phys. Chem. Chem. Phys.*, 2017, **19**, 9402–9408.
39 A. Volk, D. Knez, P. Thaler, A. W. Hauser, W. Grogger, F. Hofer and W. E. Ernst, *Phys. Chem. Chem. Phys.*, 2015, **17**, 24570–24575.
40 C. Hébert, M. Willinger, D. S. Su, P. Pongratz, P. Schattschneider and R. Schlögl, *Eur. Phys. J. B*, 2002, **28**, 407–414.
41 J. Li, B. Gauntt, J. Kulik and E. Dickey, *Microsc. Microanal.*, 2009, **15**, 1004–1005.
42 X. Lin, Y. Wang, V. P. Dravid, P. Michalakos and M. Kung, *Phys. Rev. B: Condens. Matter Mater. Phys.*, 1993, **47**, 3477.
43 M. Melzer, J. Urban, H. Sack-Kongehl, K. Weiss, H.-J. Freund and R. Schlögl, *Catal. Lett.*, 2002, **81**, 219–221.
44 Y. Li, J.-L. Kuang, Y. Lu and W.-B. Cao, *Acta Metall. Sin. (Engl. Lett.)*, 2017, **30**, 1017–1026.
45 W. Zachariasen, *Geol. Foeren. Stockholm Foerh.*, 1929, **51**, 123.
46 P. Dernier, *Mater. Res. Bull.*, 1974, **9**, 955–963.
47 N. Schoenberg, *Acta Chem. Scand.*, 1954, **8**, 221–225.
48 R. Wyckoff, *Crystal Structures*, J. Wiley and Sons, New York, NY, USA, 1964, vol. 2.
49 J. Ketelaar, *Nature*, 1936, **137**, 316.
50 K. Momma and F. Izumi, *J. Appl. Crystallogr.*, 2011, **44**, 1272–1276.
51 C. Ramana, O. Hussain, B. S. Naidu and P. Reddy, *Thin Solid Films*, 1997, **305**, 219–226.
52 H.-J. Zhai, J. Döbler, J. Sauer and L.-S. Wang, *J. Am. Chem. Soc.*, 2007, **129**, 13270–13276.